Solution and Crystal Structure of Cytisine, a Quinolizidine Alkaloid

Paolo Mascagni,* Marika Christodoulou, and William A. Gibbons *
Department of Pharmaceutical Chemistry, School of Pharmacy, University of London, 29/39 Brunswick Square, London WC1N 1AX
Kaleab Asres and J. David Phillipson
Department of Pharmacognosy, School of Pharmacy, University of London, 29/39 Brunswick Square, London WC1N 1AX
Neri Niccolai and Stefano Mangani *
Department of Chemistry, University of Siena, 53100 Siena, Italy

The solution and crystal structure of the alkaloid cytisine has been studied using n.m.r. techniques and *X*-ray crystallography respectively. ^1H and ^{13}C relaxation parameters and coupling constants have been used to (i) study the motion of cytisine in solution and (ii) measure interatomic distance and dihedral angles. Agreement, within experimental error, has been found between the solution and crystal parameters.

Quinolizidine alkaloids are polycyclic molecules well known for their toxicity to man and livestock.[1] Among these alkaloids, cytisine (**1**), which contains a pyridone moiety, is more acutely toxic than the corresponding saturated alkaloids and its toxicological responses include nausea, convulsions, and death by respiratory failure. The structure of cytisine has been elucidated by chemical degradation and by synthesis.[2,3]

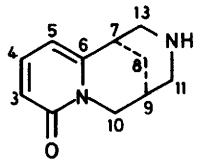

(**1**)

In this paper we have undertaken a detailed analysis of the structure and conformation of cytisine in the solution and solid state as part of a wider programme on isolation, structure, conformation, and structure–activity relationships of this class of alkaloids. Conformational and dynamic parameters of cytisine in chloroform solutions were obtained, according to an approach successfully used for other classes of natural compounds,[4] from studies of carbon and proton relaxation parameters. The results were then correlated with the crystal structure of cytisine.

Experimental

Cytisine was purchased from Koch–Light Laboratories and purified by recrystallization from benzene–hexane; the same solvent system was used to obtain crystals of cytisine for *X*-ray crystallography. The optical activity of cytisine was measured in ethanol, $[\alpha]_D^{25}$ −119.9°, identical with the value in the literature.[3]

N.m.r.—Purified cytisine (5 mg) was dissolved in $CDCl_3$ (1 ml) and the solution bubbled with nitrogen.

1D N.m.r. spectra were taken on a Varian XL-300 instrument and the Bruker AM-500 instrument at the M.R.C. Centre at Mill Hill. ^{13}C Relaxation measurements were also recorded on a Bruker WP-80-SY instrument.

2D N.m.r. experiments were performed only on the Varian instrument. 2D-COSY and 2D-COSY-45 experiments were run using the *t*-90-τ-Pw-Acq pulse sequence with Pw 90 and 45°, respectively.[5] 512 Increments of 1 024 data points were taken in each case and the matrix thus obtained symmetrized with respect to the diagonal.

The 2D NOESY pulse sequence was modified according to a recent paper,[6] in order to remove any residual scalar coupling constant contributions. The mixing time was 0.2 s.

Classical 2D-*J*-resolved and ^1H–^{13}C correlation spectra[7,8] were run using 128 increments of 2 048 points in both cases.

Non-selective proton and carbon spin–lattice relaxation were measured with the inversion recovery method.

The selective spin–lattice relaxation rates were obtained by selectively inverting the proton magnetization with the decoupler channel and monitoring the recovery of the magnetization to equilibrium. Typical values for the 90° pulse from the decoupler channel were *ca.* 15 ms.

Quantitative, monodimensional n.O.e.s were obtained with 5—10 s pre-irradiation of the proton of interest followed by acquisition. The interval between acquisitions was set at 20 s.

The gating of the decoupler channel prior to acquisition generated broad-band decoupled ^{13}C spectra with no Overhauser enhancement. Subtraction of these spectra from those obtained with no decoupler gating yielded the $n.O.e._{BB}$.

X-Ray Crystallography.—The *X*-ray data were taken at the Department of General and Inorganic Chemistry, University of Florence, Florence.

(a) *Data collection.* Unit-cell parameters and other crystal data are reported in Table 1.

A clean fragment of a colourless prismatic crystal was mounted on a Phillips PW1100 automatic diffractometer; graphite-monochromatized Mo-K_α radiation was used for measuring both cell dimensions and diffraction intensities. A least-squares fit of 25 carefully centred reflections was used to determine cell constants.

The quadrant of reciprocal space $\pm hkl$ was inspected in the range $5° \leqslant 2\theta \leqslant 40°$ and equivalent reflections were merged to give 1 081 independent intensities.

The θ–2θ scan technique was used with a scan speed of $0.08°/s^{-1}$ and a variable scan width of 1.1 + 0.3 tang (θ)°. At each end of the scan range the background was counted half the total scan time. The intensities of three control reflections, monitored every 120 min, did not show any systematic variation. Data were corrected for Lorentz and polarization effects; absorption corrections were not applied.

The 708 reflections with intensities greater than $2.5\sigma(I)$ were used for the structure solution and refinement. The standard

Table 1. Crystal data for cytisine

Mol. formula	$C_{11}H_{14}N_2O$
Space group	$P2_12_12_1$
Crystal size	0.5 × 0.2 × 0.1 mm
a	9.978(5) Å
b	26.615(8) Å
c	7.217(4) Å
V	1 916.6 Å^3
Z	8
$F(000)$	816
Radiation	Mo-K_α (λ 0.7093 Å)
μ(Mo-K_α)	0.25 cm^{-1}
Molecular weight	190.2
$D_{calc.}$	1.32 g cm^{-3}
R^a	0.051
$R_w{}^b$	0.047

^{a} $R = \Sigma[|F_o| - |F_c|]/\Sigma[F_o]$. ^{b} $R_w = [\Sigma_w(|F_o| - |F_c|)^2/\Sigma_w(F_o)^2]^{\frac{1}{2}}$.

deviation of intensity $\sigma(I)$ was computed as $[P + B_1 + B_2 + (0.031)^2]^{\frac{1}{2}}$ where P is the total integrated count, B_1 and B_2 are the background counts, I is the peak intensity after subtraction of the background, and 0.031 is a correction for unrealistically small standard deviations in strong reflections.

The space group $P2_12_12_1$ was determined on the basis of systematic absences.

(b) *Structure solution and refinement.* The structure of cytisine was solved by direct methods provided by the SHELX76 set of programs.[9]

Origins, enantiomorph, and multisolution phases were chosen from reflections at the top of the convergence map. The E map with the third best figure of merit showed a recognizable fragment of both molecules in the asymmetric unit. A subsequent Fourier map revealed the rest of the nonhydrogen atoms.

Two full-matrix least-squares cycles with isotropic temperature factors for all the atoms reduced R to 0.085. Successive difference electron density syntheses revealed all the hydrogen atoms. In the following cycles only the two hydrogen atoms bonded to the N(12) atoms were allowed to refine, the remainder were introduced in calculated positions, and constrained to ride on their carbon atom (C–H distance 1.08 Å).

Refinement converged to $R = 0.051$ and $R_w = 0.047$ [the function minimized was $\Sigma w(|F_o| - |F_c|)^2$ with weights $w = k/\sigma^2(F)$, $k = 1.0974$ in the last cycle]. In the last cycle of isotropic refinement the shift:e.s.d. ratio was well below unity for all parameters. A final difference synthesis was featureless. All calculations were performed with the SHELX76 set of programs which uses the analytical approximation for the atomic scattering factors taken from ref. 10. Plots were made by the ORTEP program.[11]

Results and Discussion

^{1}H *N.m.r. Assignments.*—Spectra of solutions of cytisine in deuterochloroform were taken at 300 and 500 MHz. The assignment of the proton spectrum was obtained by ^{1}H–^{1}H chemical shift correlation and by two-dimensional n.O.e. spectroscopy. A complete list of the proton assignments is given in Table 2; some of them are discussed here.

The *exo*- and *endo*-8-H resonances overlapped at δ 1.68. The lack of the expected non-equivalence for these two protons was attributed to N-12 inversion, whereby the attached proton moves from the axial to the equatorial position with rates which range between 10^4 and 10^5 s^{-1}.[12] The spectrum of the protonated form of cytisine was consistent with this conclusion.

Table 2. Proton chemical shifts, configurations, and relaxation parameters of cytisine in chloroform solution

	δ[a]	Configuration[b]	R_{NS}[c]	R_{SE}[d]	F_i[e]
3-H	6.18		0.14	0.10	1.33
4-H	7.02		0.19	0.14	1.30
5-H	5.73		0.25	0.19	1.31
7-H	2.69	e(α)	0.41	0.31	1.32
8-H	1.68		0.91	0.69[f]	1.35
8-H	1.68		0.91	0.69[f]	1.35
9-H	2.05	e(α)	0.48	0.36	1.33
10-H(d)	3.85	e(β)	0.73	0.53	1.38
10-H(u)	3.62	a(α)	0.73	0.52	1.40
11-H(d)	2.83	e(β)	0.91	0.69	1.32
11-H(u)	2.72	a(α)			
N–H	1.17				
13-H(d)	2.79	a(α)			
13-H(u)	2.74	e(β)			

[a] Chemical shifts refer to Me_4Si. [b] a = axial; e = equatorial; β = above the plane; α = below the plane. [c] $R_{NS} = 1/T_1^{NS}$; non-selective relaxation rates in s^{-1}. [d] $R_{SE} = 1/T_1^{SE}$; selective relaxation rates in s^{-1}. [e] $F_i = R_{NS}/R_{SE}$; see text for discussion. [f] R_{SE} for 8-H_2 were calculated from σ_{gem} (see text).

Thus the quaternization of N-12 with CF_3COOH removed the degeneracy of the two 8-H_2 and permitted the measurement of their geminal coupling constant (see Table 8).

The proton signal at δ 3.85 was a doublet in contrast to the three correlations seen in the contour plot of the COSY experiment. This proton signal was thus assigned to the methylene group (C-10) coupling with the vicinal 9-H; geometrical considerations indicated that a four-bond coupling takes place with one 8-H_2. Although the two-dimensional experiment revealed all these couplings, no further splitting than that caused by the geminal interaction was seen in the spectrum of cytisine, nor in that of its trifluoroacetate salt. The signal linewidth was hence used to provide an upper limit for the coupling constants of 10- with 8- and 9-H: these were 0.8 Hz. Most of the remaining coupling constants were assigned directly from the 1D n.m.r. traces. In some instances (*e.g.* 11- and 13-H overlap at δ *ca.* 2), the assignment was made from the appropriate 2D–J projections. The experimentally derived J values were then refined by computer simulation and the corrected values listed in Table 8. Of particular interest were the long-range couplings involving proton pairs [10 (u); (11) (d)], [10 (d); 8], [9; 7], and [13 (u); 8], which, when used in combination with molecular models, yielded the geometry of several fragments of the molecule. For instance the coupling constant of 1.3 Hz between 13-(u) and 8-H indicated that the two protons had 'a planar zigzag or W arrangement'[13] consistent only with an equatorial (β) conformation for 13-H(u). 10-(u) and 11-H(u) were instead both axial and α as indicated by the long-range coupling of 1.3 Hz.

The complete assignment of the proton configurations by means of J coupling constants is shown in Table 2.

^{13}C *Assignments.*—2D N.m.r. heteronuclear correlation spectroscopy was used to assign all the protonated carbon signals of cytisine; the carbon carbonyl and the quaternary C-6 were assigned on the basis of their chemical shifts. Our assignment agreed with that reported in the literature.[14]

^{13}C *Relaxation Measurements.*—^{13}C Spin–lattice relaxation rates of protonated carbons can be analysed in terms of molecular dynamics provided the carbon nuclei fully relax

Table 3. ^{13}C Chemical shifts and relaxation parameters for cytisine in chloroform solution

	δ (p.p.m.)[a]	R_1[b]	R_1[c]	n.O.e.$_{BB}$[d]
C-2	163.6			0.26
C-3	116.6	0.44	0.34	1.75
C-4	138.7	0.37	0.31	2.00
C-5	104.9	0.34	0.29	2.00
C-6	151.1			0.4
C-7	35.6	0.36	0.30	2.00
C-8	26.3	0.37	0.27	2.00
C-9	27.7	0.33	0.31	2.00
C-10	49.7	0.36	0.27	2.00
C-11	54.0	0.34	0.29	1.93
C-13	53.0	0.32	0.27	1.88

[a] Chemical shifts refer to Me_4Si. [b] $R_1 = 1/T_1$; rates were measured at the spectrometry frequency of 75 MHz for carbon. [c] Relaxation rates were measured at the frequency of 20 MHz for ^{13}C. [d] N.O.e.$_{BB}$ were measured at a field of 75 MHz for carbon. They are ±0.1.

through dipolar mechanism with their directly attached protons.[15] The broad-band ^1H–^{13}C nuclear Overhauser effect, n.O.e.$_{BB}$, is a measure of the effectiveness of the dipolar interaction.[16] When the n.O.e.$_{BB}$ were measured for cytisine we found (Table 3) that, with the exception of C-3, whose n.O.e.$_{BB}$ is 1.71, all protonated carbons had Overhauser contributions of 2.0 ± 0.1, proving that the dipolar interaction is the sole mechanism of relaxation for these carbons and that the molecular rotation is sufficiently fast so that the 'extreme narrowing limit' $[(w_H + w_C)^2 t_c^2 \ll 1]$ applies.

The ^{13}C spin–lattice relaxation rates were obtained at two different spectrometer frequencies, 75 and 20 MHz respectively. When corrected for the number of protons directly bonded the rates of all the protonated carbons were very similar at both frequencies; at 75 MHz all the rates ranged from 0.37 s^{-1} for C-4 to 0.32 s^{-1} for C-13 with the exception of C-3 which had a relaxation rate of 0.44 s^{-1}, the average value, calculated without taking into account the largest rate, being 0.32 s^{-1}; at 20 MHz the mean relaxation rate was 0.29 s^{-1} and also in this case the largest value was recorded for C-3 (0.34 s^{-1}) (Table 3). In general the relaxation rate data confirmed the conclusions from the non-selective Overhauser effects. The virtually identical mean relaxation rates at the two spectrometer frequencies indicated that (i) the carbon nuclei relax completely by dipolar interactions, and (ii) the latter are modulated by molecular motions within the extreme narrowing conditions.[16]

Relaxation mechanisms other than dipolar probably account for the anomalous behaviour of C-3 but this does not alter the conclusion that cytisine behaves in solution like a rigid isotropic rotor. The measured spin–lattice relaxation rates of all protonated carbons, with the exception of C-3, were therefore analysed using equation (1)[15] and the effective correlation time

$$1/T_1 = \hbar^2\gamma_H^2\gamma^2{}_C r^{-6}\tau_c \qquad (1)$$

calculated for each C–H vector of cytisine. The narrow range of values obtained, τ_c 1.50 ± 0.2 × 10^{-11} s, confirmed that a single correlation time accounted for the fast molecular tumbling. As expected, the inversion process at N-12, with typical rates of 10^4—10^5 s^{-1}, did not contribute to the relaxation process.

^1H Relaxation Measurements.—The dipolar contribution to the proton relaxation rates was estimated from non-selective and selective spin–lattice relaxation time measurements. For a spin *i*, in a multiple spin system at thermal equilibrium, the overall relaxation rate is expressed[17] by equation (2) where σ is

Table 4. ^1H–^1H Distances of cytisine from Overhauser effects and *X*-ray crystallography

Observed ^1H	Irradiated ^1H	n.O.e. (%)	σ[a]	$r_{n.O.e.}$[b]	$r_{X\text{-ray}}$[c]
3-H	4-H	17.8	1.6	2.54	2.46 (2.38)
5-H	4-H	11.2	2.3	2.39	2.49 (2.49)
3-H	5-H	−2.9		4.45	4.28 (4.24)
4-H	5-H	19.1	2.7	2.33	2.49 (2.49)
5-H	3-H	−3.0			4.28 (4.24)
4-H	3-H	13.2	1.8	2.48	2.46 (2.38)
9-H	11-H(d)	4.9	1.8	2.49	2.44 (2.42)
10-H(d)	11-H(d)	5.0	2.6	2.34	2.39 (2.38)
10-H(d)	9-H	2.9	1.5	2.56	2.61 (2.55)
11-H(d)	9-H	5.0	3.4	2.24	2.44 (2.42)
10-H(u)	9-H	7.3	3.7	2.21	2.26 (2.28)
11-H(u)	9-H	3.6			2.43 (2.38)
8-H	9-H	2.15	1.5	2.56	2.48 (2.50)
11-H(d)	10-H(d)	5.0			2.39 (2.38)
5-H	7-H	11.2	2.3	2.40	2.34 (2.46)
7-H	5-H	8.5	2.6	2.34	2.34 (2.46)
8-H	7-H	3.4	2.3	2.39	2.49 (2.53)

[a] σ Values were calculated from the Overhauser effects and the selective relaxation rates from Table 1. Values are in s × 10^{-2}. [b] Distances in Å: they were calculated using equations (3) and (4) for the positive and negative n.O.e.s respectively and a correlation time of 1.5 × 10^{-11} s. [c] Interproton distances (Å) from *X*-ray data; figures in parentheses refer to the second structure of cytisine (see text).

$$R_i^{(NS)} = \sum_{i \neq j,m} R_{j,i}^m + \sum_{i \neq j} \sigma_{ij} \qquad (2)$$

the cross-relaxation rate between the dipolarly coupled spins *i* and *j* and the first term on the right of the equation accounts for several relaxation contributions such as intramolecular and intermolecular dipole–dipole, spin rotation, chemical shift anisotropy, and scalar coupling. Freeman and his co-workers[18] have shown that this term equals the relaxation rate measured under selective excitation conditions (R_i^{SE}). Furthermore, if the relaxation of spin *i* is solely by dipolar coupling to spin *j* and the system is in the fast motion limits, then the ratio of the observed rates is given by equations (3) where $\rho_{ij} = W_0^{ij} + 2W_i^{ij} +$

$$F_i = R_i^{NS}/R_i^{SE} = \sigma_{ij}/\rho_{ij} = 1.5 \qquad (3)$$

W_2^{ij} and W_i, W_0, and W_2 refer to the transition probabilities of the dipole–dipole relaxation mechanism.

With the exception of N–H and 8-H_2 all protons of cytisine had F_i ratios between 1.3 and 1.4 (Table 2). The lower value for 8-H_2 (1.18) was ascribed to spectral overlap of these two protons. Thus when 8-H_2 are irradiated, although the σ_{ij} terms cancel, the cross-relaxation contribution from the inter-methylene dipolar interaction (σ_{gem}) is still contained in the expression of the relaxation rate. We can then write equation (4)

$$R^{SE}(CH_2) = R^x(CH_2) + \sigma_{gem} \qquad (4)$$

where the first term on the right of the equation refers to the effective relaxation rate. On the reasonable assumption that an average $F = 1.35$ can be applied to 8-H_2, the R^x rate and σ_{gem} was calculated using the experimental non-selective ratio of 0.91 s^{-1}. The knowledge of the geminal cross-relaxation rate therefore permitted an independent evaluation of the correlation time. This was 1.15 × 10^{-11} s, a value close to that calculated directly from ^{13}C relaxation parameters.

The dipolar interaction between the ^{14}N and its directly bonded proton as well as the nitrogen inversion could account for the low F(N–H) ratio; the effects of the first interaction are well documented [19] while chemical exchange made it difficult to invert selectively the N–H proton magnetization.

In conclusion it seems appropriate to use an F_i ratio of 1.35 to describe the relaxation behaviour of the protons of cytisine. The deviation from 1.5 could be accounted for by relaxation mechanisms other than dipolar or by slow motion in solution. The former conclusion applies to our system since the ^{13}C relaxation parameters demonstrated that the fast-motion limits do apply in the case of cytisine.

^1H–^1H *Overhauser Effects.*—Long, low-power selective irradiations were used to measure n.O.e.s quantitatively. Two classes of n.O.e.s were recorded: negative n.O.e.s between 3- and 5-H and positive ones at all other protons. The experimental results are shown in Table 4 and were used to calculate interproton distances as described in the following section.

Some of the n.O.e.s from Table 3 were also used for an independent calculation of the correlation time. For instance, the Overhauser effect at spins 3 and 5 observed after irradiation of H-4 (see Table 4) when used with the appropriate relaxation rates and *X*-ray distances yielded τ_{3-4} 1.25 × 10^{-11} and τ_{4-5} 1.55 × 10^{-11} s, identical, within the experimental error, with that calculated using the ^{13}C relaxation parameters.

Interproton Distances from N.m.r. Parameters.—The negative n.O.e.s observed for 3- and 5-H were rationalized in terms of 'linear three spin system (obtuse case)'.[17] Thus Noggle has shown that for such a system the effect recorded at an end spin (a) while the other end spin (c) is saturated has a negative sign and that, if the correlation time is constant over the entire system, the interproton distances separating the three spins (a—c) can be measured using the formula (5). Here $f_i(j)$ is the

$$(r_{a-c})^6/(r_{a-b})^6 = f_a(b) + [f_a(c)f_c(b)]/f_a(c) + [f_a(b)f_b(c)] \quad (5)$$

fractional Overhauser effect. From equation (5) one of the distances can be calculated if the other is known. In cytisine 3-, 4-, and 5-H lie on the same plane, hence r_{3-4} can be calculated from standard interatomic distances: using r_{3-4} 2.4 Å and equation (5) we obtained r_{3-5} 4.4 Å in good agreement with the crystallographic figure of 4.29 Å (see text below).

Using the selective relaxation rates from Table 2 and the n.O.e.s from Table 3 cross-relaxation rates (σ) were derived according to equation (6).[17] The σ values thus obtained were

$$\sigma_{ij} = R^{SE}\,\text{n.O.e.}_i(j) \quad (6)$$

$$\sigma_{ij} = (\text{const})(1/r_{ij}^6)(\tau_c) \quad (7)$$

then used to calculate interatomic distances using equation (7). The calculated distances are shown in Table 4.

Crystal Structure.—The crystal structure of cytisine is depicted in two forms in Figure 2. Positional parameters of the atoms are listed in Table 5. Figure 2 shows a perspective view of

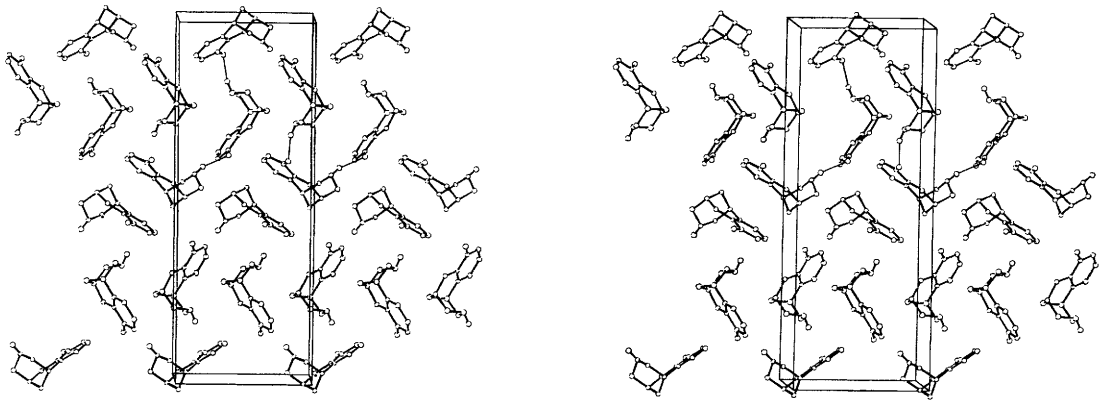

Figure 1. Stereoview approximately down *c* axis of the molecular packing. Hydrogen bonds are shown only for the two molecules of an asymmetric unit

Table 5. Positional parameters and their e.s.d.s for the two independent molecules of cytisine in the unit cell

Atom	*x*	*y*	*z*	Atom	*x*	*y*	*z*
N(1)	0.132 9(7)	0.561 8(2)	0.479 0(9)	N(1′)	0.560 8(7)	0.692 2(3)	0.107 9(10)
O(2)	0.173 3(6)	0.594 5(2)	0.191 2(9)	O(2′)	0.627 0(6)	0.629 9(2)	−0.089 3(9)
C(2)	0.210 4(9)	0.591 7(4)	0.354 6(13)	C(2′)	0.634 5(10)	0.648 3(3)	0.069 0(14)
C(3)	0.325 3(10)	0.614 7(3)	0.429 9(14)	C(3′)	0.712 9(9)	0.629 3(3)	0.219 6(13)
C(4)	0.359 2(10)	0.608 8(3)	0.616 0(13)	C(4′)	0.715 8(10)	0.651 7(3)	0.384 4(15)
C(5)	0.277 4(9)	0.579 7(3)	0.732 0(14)	C(5′)	0.643 0(9)	0.696 3(4)	0.417 2(14)
C(6)	0.166 3(9)	0.557 2(3)	0.662 5(13)	C(6′)	0.564 4(9)	0.715 4(3)	0.277 0(13)
C(7)	0.080 8(9)	0.524 3(3)	0.786 5(13)	C(7′)	0.482 6(9)	0.763 2(4)	0.308 9(14)
C(8)	0.025 9(9)	0.480 4(3)	0.670 4(11)	C(8′)	0.359 1(10)	0.762 9(4)	0.182 7(12)
C(9)	−0.064 7(9)	0.501 9(3)	0.521 4(13)	C(9′)	0.408 0(10)	0.760 7(3)	−0.013 8(13)
C(10)	0.017 2(9)	0.535 5(3)	0.389 6(12)	C(10′)	0.477 6(9)	0.710 9(3)	−0.046 9(13)
C(11)	−0.180 5(9)	0.530 1(3)	0.612 5(13)	C(11′)	0.495 9(9)	0.806 3(4)	−0.058 9(14)
N(12)	−0.128 2(7)	0.571 9(3)	0.723 2(11)	N(12′)	0.611 3(9)	0.807 7(3)	0.067 6(12)
H(1)	−0.184 9(97)	0.954 9(38)	0.816 5(151)	H(1′)	0.648 9(119)	0.839 3(42)	0.058 6(177)
C(13)	−0.036 7(9)	0.553 6(3)	0.871 4(13)	C(13′)	0.569 9(10)	0.809 5(3)	0.259 6(13)

Table 6. Interatomic distances (A) and angles (°) and their e.s.d.s for the two independent molecules of cytisine in the unit cell

N(1)–C(2)	1.428(10)	N(1)–C(6)	1.371(10)
N(1)–C(10)	1.495(10)	O(2)–C(2)	1.239(9)
C(2)–C(3)	1.408(11)	C(3)–C(4)	1.394(13)
C(4)–C(5)	1.402(11)	C(5)–C(6)	1.356(11)
C(6)–C(7)	1.516(11)	C(7)–C(8)	1.538(10)
C(7)–C(13)	1.536(11)	C(8)–C(9)	1.517(11)
C(9)–C(10)	1.542(11)	C(9)–C(11)	1.527(11)
C(11)–N(12)	1.466(10)	N(12)–H(1)	1.071(111)
N(12)–C(13)	1.488(10)	N(1′)–C(2′)	1.408(10)
N(1′)–C(6′)	1.369(10)	N(1′)–C(10′)	1.478(10)
O(2′)–C(2′)	1.245(10)	C(2′)–C(3′)	1.432(12)
C(3′)–C(4′)	1.332(11)	C(4′)–C(5′)	1.410(11)
C(5′)–C(6′)	1.379(12)	C(6′)–C(7′)	1.528(12)
C(7′)–C(8′)	1.532(12)	C(7′)–C(13′)	1.550(12)
C(8′)–C(9′)	1.501(12)	C(9′)–C(10′)	1.516(11)
C(9′)–C(11′)	1.532(12)	C(11′)–N(12′)	1.470(11)
N(12′)–N(1′)	0.924(114)	N(12′)–C(13′)	1.447(12)
C(2)–N(1)–C(6)	121.6(8)	C(2)–N(1)–C(10)	114.0(7)
C(6)–N(1)–C(10)	124.3(8)	O(2)–C(2)–N(1)	118.0(9)
O(2)–C(2)–C(3)	125.8(10)	N(1)–C(2)–C(3)	116.2(9)
C(2)–C(3)–C(4)	121.3(10)	C(3)–C(4)–C(5)	119.8(10)
C(4)–C(5)–C(6)	119.9(9)	N(1)–C(6)–C(5)	121.1(9)
N(1)–C(6)–C(7)	119.0(8)	C(5)–C(6)–C(7)	119.8(9)
C(6)–C(7)–C(8)	108.6(7)	C(6)–C(7)–C(13)	111.7(7)
C(8)–C(7)–C(13)	109.4(7)	C(7)–C(8)–C(9)	108.2(7)
C(8)–C(9)–C(10)	109.9(7)	C(8)–C(9)–C(11)	109.4(7)
C(10)–C(9)–C(11)	112.4(7)	N(1)–C(10)–C(9)	114.5(7)
C(9)–C(11)–N(12)	109.8(7)	C(11)–N(12)–C(13)	111.2(7)
C(11)–N(12)–H(1)	125.9(51)	C(13)–N(12)–H(1)	93.4(53)
C(7)–C(13)–N(12)	110.3(8)		
C(2′)–N(1′)–C(6′)	122.6(8)	C(2′)–N(1′)–C(10′)	115.0(7)
C(6′)–N(1′)–C(10′)	122.4(7)	O(2′)–C(2′)–N(1′)	118.5(9)
O(2′)–C(2′)–C(3′)	126.2(9)	N(1′)–C(2′)–C(3′)	115.3(8)
C(2′)–C(3′)–C(4′)	122.1(9)	C(3′)–C(4′)–C(5′)	121.1(10)
C(4′)–C(5′)–C(6′)	118.8(10)	N(1′)–C(6′)–C(5′)	120.1(8)
N(1′)–C(6′)–C(7′)	119.8(9)	C(5′)–C(6′)–C(7′)	120.1(9)
C(6′)–C(7′)–C(8′)	109.6(9)	C(6′)–C(7′)–C(13′)	109.8(7)
C(8′)–C(7′)–C(13′)	108.7(8)	C(7′)–C(8′)–C(9′)	107.5(8)
C(8′)–C(9′)–C(10′)	109.3(8)	C(8′)–C(9′)–C(11′)	110.9(8)
C(10′)–C(9′)–C(11′)	113.4(8)	N(1′)–C(10′)–C(9′)	115.6(8)
C(9′)–C(11′)–N(12′)	109.6(8)	C(11′)–N(12′)–C(13′)	111.8(8)
C(11′)–N(12′)–H(1′)	107.3(77)	C(13′)–N(12′)–H(1′)	98.8(81)
C(7′)–C(13′)–N(12′)	110.8(8)		

Table 7. Least-squares planes and atomic deviations from the planes of cytisine

Least-squares planes

Equations to planes (expressed in terms of an orthogonal axis system: a, b, c^* coefficients are in Å units)

Plane A: $-0.544\,35X + 0.807\,81Y + 0.226\,11Z = 12.149\,65$

Plane A′: $0.775\,27X + 0.553\,03Y - 0.305\,15Z = 12.090\,00$

Plane C: $0.282\,69X + 0.828\,49Y - 0.483\,41Z = 9.053\,93$

Plane C′: $-0.762\,25X + 0.607\,08Y + 0.224\,56Z = 10.783\,95$

Deviations of atoms from the planes (Å)

Plane	N(1) N(1′)	C(2) C(2′)	C(3) C(3′)	C(4) C(4′)	C(5) C(5′)	C(6) C(6′)	C(7) C(7′)	C(9) C(9′)	C(11) (C11′)	C(13) C(13′)	O(2) O(2′)	C(10) C(10′)
A	−0.012	0.008	0.002	−0.007	0.002	0.008	−0.033*	−0.157*			0.003*	−0.094*
A′	−0.003	0.006	0.001	−0.009	0.011	−0.006	−0.006*	0.091*			0.025*	−0.032*
C							−0.010	0.010	−0.010	0.010		
C′							−0.002	0.002	−0.002	0.002		

* Atoms not included in least-square plane calculation.

Table 8. ^1H–^1H coupling constants and dihedral angles of cytisine

^1H–^1H	J/Hz	θ_J[a]	X-Ray[b]
3–5	1.41		−0.14 (−2.24)
3–4	9.49		0.96 (0.49)
4–5	7.06		−1.04 (−1.82)
7–8	2.54	53	63.5 (60.20)
7–8′	2.54	53	−59.65 (−60.23)
7–13(u)	2.42	54	58.94 (58.37)
7–13(d)	2.42	54	−60.87 (−60.47)
13(u)–13(d)	12.09		
8–8′	15.00[c]		
8–9	2.5	53	58.36 (57.23)
8′–9	2.5	53	−62.23 (−63.36)
9–10(u)	7.62	19	30.78 (38.13)
9–10(d)	0.8	73	−87.75 (−80.25)
10(d)–8	0.8	17	−27.39 (−46.55)
10(u)–11(u)	1.25	28	−24.87 (−16.15)
10(u)–10(d)	15.63		
9–11(u)	2.23	55	58.77 (62.04)
9–11(d)	2.35	54	−61.35 (−57.48)
11(u)–11(d)	12.60		
11(d)–8	0.91	25	−2.63 (2.98)
13(u)–8	1.29	28	0.00 (−0.61)

[a] Dihedral angles (°) from J coupling constants.[12] [b] Dihedral angles (°) from X-ray data. Figures in parentheses refer to the second crystal structure of cytisine. [c] J_{8-8} Obtained from the spectrum of cytisine trifluoroacetate.

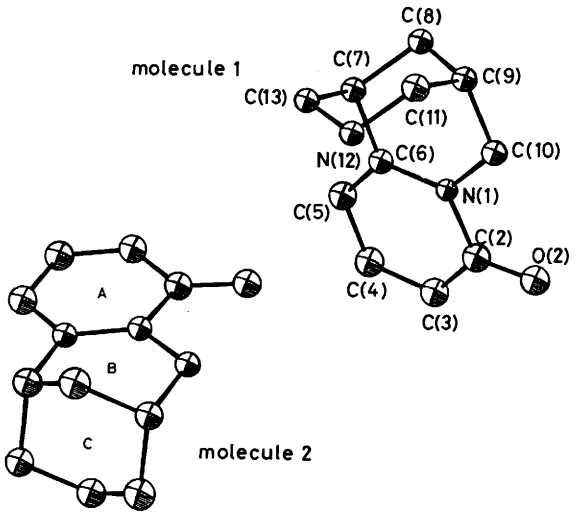

Figure 2. ORTEP drawing of the two independent molecules. Thermal ellipsoids are drawn at 30% probability. Hydrogen atoms are omitted for clarity

the two independent molecules in the asymmetric unit and the lettering scheme. Bond lengths and angles are reported in Table 6. With the exception of 12-H, the fractional atomic co-ordinates for all the other hydrogen atoms were obtained from calculated positions and hence the relative interproton distances of Table 4 were affected by an error which was estimated to be ±0.15 Å.

Both independent molecules show an identical conformation. The A ring of cytisine is planar and bond lengths and angles give evidence of a considerable delocalization of electrons on the ring. The oxygen atom lies in the plane of C-7, C-9, and C-10 of ring B which is in the half-chair conformation (the maximum deviation from the mean plane of ring A is shown by C-9: 0.15 and 0.10 Å for C-9 and C-9′, respectively).

Least-squares planes with atomic deviations are listed in Table 7. Ring C exhibits a rigid chair conformation with C-7, C-9, C-11, and C-13 of both molecules lying in a plane. The latter makes an angle of 66.0 and 71.1° with the A ring respectively in the two molecules.

The two independent molecules in the asymmetric unit are in perpendicular positions in respect to each other, the A and A′ planes being 87.5° apart. In the lattice, cytisine molecules are linked together by the intramolecular hydrogen bonds shown in Figure 1. Each molecule makes two hydrogen bonds of the type: O-2(x, y, z)–N-12′ ($= +x, = -y, 1 - z$) at a distance of 3.23 Å and N-12(x, y, z)–O-2′($1 + x, y, z$) at a distance of 3.20 Å.

Solution Conformation of Cytisine.—Molecular modelling based upon the interproton distances obtained from the n.m.r. measurements yielded a conformation for cytisine similar to that obtained from the X-ray data for the skeleton. This allowed us to discriminate between the different dihedral angles obtained for individual H–(C–C)$_n$–H moieties from J coupling constants.[20] A correlation of the latter with their respective angles θ is shown in Table 8 where the crystal angles are added for comparison purposes.

Conclusions.—The conformation that cytisine adopts in solution and in solid state has been investigated using the data from relaxation parameters and X-ray crystallography, respectively. Results from the two sets of data indicate that in both phases the three rings of the alkaloid have a planar, half-chair and chair conformation respectively, with 12-H switching from an α to a β orientation in the solution structure. In solution, cytisine behaves like a rigid rotor whose motion and individual proton and carbon relaxation rates are modulated by a unique correlation time. The magnitude of the latter was calculated using several independent methods and is consistent with an overall fast tumbling rate of $6.7 \pm 0.2 \times 10^{10}$ s^{-1}. The net of hydrogen-bonding seen in the lattice of the cytisine crystals was not detected in the solution phase, except, perhaps, at higher concentrations. Thus the relaxation figures for the carbons atoms obtained at concentrations in the 0.1M range, although very similar to those obtained for low concentrations, were not always reproducible. This reflects aggregation in solution which would then have considerable effects on the motion and hence on the spin–lattice relaxation rates.

References

1 G. A. Cordell, 'An Introduction to Alkaloids: a Bioenergetic Approach,' Wiley, New York, 1981.
2 F. Bohlmann, A. Englisch, N. Ottawa, H. Sander, and W. Weise, *Angew. Chem.*, 1955, **67**, 708.
3 S. Okuda, K. Tsuda, and H. Kataoka, *Chem. Ind. (London)*, 1961, 1751 and references therein.
4 (*a*) C. R. Jones, C. T. Sikakana, S. P. Hehir, M. Kuo, and W. A. Gibbons, *Biophys. J.*, 1978, **24**, 815; (*b*) P. Mascagni, N. Niccolai, D. H. Rich, and W. A. Gibbons, *J. Chem. Soc., Perkin Trans. 1*, 1985, 245; (*c*) P. Mascagni, N. Niccolai, A. Prugnola, and W. A. Gibbons, *J. Chem. Soc., Perkin Trans. 2*, 1986, 1015.
5 W. P. Aue, E. Bartholdi, and R. R. Ernst, *J. Chem. Phys.*, 1976, **26**, 133.
6 M. Rance, G. Bodenhausen, G. Wagner, K. Wuthrich, and R. R. Ernst, *J. Magn. Reson.*, 1984, **62**, 497.
7 W. P. Aue, J. Karhan, and R. R. Ernst, *J. Chem. Phys.*, 1976, **26**, 133.
8 A. Bax, R. Freeman, and S. P. Kempsell, *J. Am. Chem. Soc.*, 1980, **102**, 4839.
9 G. M. Sheldrick, 'Programs for Crystal Structure Determination,' Cambridge University, 1976.
10 'International Tables for X-Ray Crystallography,' Kynoch Press, Birmingham, 1974, vol. 4.
11 C. Johnson, ORTEP Report ORNL-3494, Oak National Laboratory, Oak Ridge, 1965.
12 F. A. L. Anet and A. J. R. Bourne, *J. Am. Chem. Soc.*, 1967, **89**, 760.

13 'Progress in Nuclear Magnetic Resonance Spectroscopy,' eds. J. W. Emsley, J. Feeney, and L. H. Sutcliffe, Pergamon Press, Oxford, 1969, vol. 5, and references therein.
14 F. Bohlmann and R. Zeisberg, *Chem. Ber.*, 1975, **108**, 1043.
15 D. Doddrell, V. Glushko, and A. Allerhand, *J. Chem. Phys.*, 1972, **56**, 3683.
16 K. F. Kuhlmann and D. M. Grant, *J. Am. Chem. Soc.*, 1968, **90**, 7355.
17 J. H. Noggle and R. E. Schirmer, 'The Nuclear Overhauser Effect,' Academic Press, New York, 1971.
18 R. Freeman, H. D. W. Hill, B. Tomlinson, and L. D. Hall, *J. Chem. Phys.*, 1974, **61**, 4466.
19 H. E. Bleich, K. R. K. Easwaran, and J. A. Glasel, *J. Magn. Reson.*, 1971, **31**, 517.
20 M. Karplus, *J. Am. Chem. Soc.*, 1963, **85**, 2870.

Received 22*nd May* 1986; *Paper* 6/893